1 April 2002

ELSEVIER

Optics Communications 204 (2002) 195–202

OPTICS COMMUNICATIONS

www.elsevier.com/locate/optcom

High energy levels and high-energetic emissions of the trivalent holmium ion in $LiYF_4$ and YF_3

Paul S. Peijzel[a,*], René T. Wegh[b], Andries Meijerink[a], Jorma Hölsä[c], Ralf-Johan Lamminmäki[c]

[a] *Department of Condensed Matter, Debye Institute, Utrecht University, P.O. Box 80 000, 3508 TA Utrecht, The Netherlands*
[b] *Philips Research Laboratories, Prof. Holstlaan 4, 5656 AA Eindhoven, The Netherlands*
[c] *Department of Chemistry, University of Turku, FIN-20014 Turku, Finland*

Received 6 December 2001; received in revised form 18 January 2002; accepted 18 January 2002

Abstract

The luminescence of $LiYF_4$ and YF_3 doped with Ho^{3+} was investigated using synchrotron radiation. In the excitation spectra transitions to previously unidentified $4f^{10}$ levels were observed thus extending the energy level diagram of Ho^{3+} into the (vacuum) ultraviolet region of the electromagnetic spectrum. Some high energy emissions were observed and could be attributed to spin forbidden $4f^9 5d \rightarrow 4f^{10}$ emissions in YF_3 and $LiYF_4$. For YF_3 doped with Ho^{3+} emission from the $^3P(1)_2$ level (situated at 63 000 cm^{-1}) was observed. Furthermore, several photon cascade emission processes were observed in which one VUV photon is converted into two or three UV/Vis photons, albeit with a low efficiency.

PACS: 71.70 Ch; 78.55 Hx; 33.20 Ni

Keywords: Vacuum ultraviolet; Rare earth ions; Holmium

1. Introduction

Spectroscopy of rare-earth (RE) ions in the vacuum ultraviolet (VUV, $\lambda < 200$ nm) has recently gained interest because of the increasing number of applications requiring VUV excitation. For generating light in the visible region of the spectrum RE ions are applied widely nowadays in for instance fluorescent tubes and fast scintillators [1]. For plasma displays and mercury-free luminescent tubes the VUV emission from a xenon discharge may be used. However, the phosphors that are used in fluorescent tubes nowadays are not optimized for VUV excitation. The efficiency of excitation in the VUV region is low and the phosphors suffer from degradation due to the high-energetic radiation. Therefore new types of phosphors should be developed [2,3]. These phosphors should also have a visible quantum efficiency above unity [4]. It was shown recently that it is

* Corresponding author. Fax: + 31-30-2532403.
E-mail address: p.s.peijzel@phys.uu.nl (P.S. Peijzel).

0030-4018/02/$ - see front matter
PII: S0030-4018(02)01195-1

possible to obtain a visible quantum efficiency of about 190% with the Gd^{3+}/Eu^{3+} quantum cutting couple [5]. For the further development of quantum cutting phosphors and for the possible application of RE ions as sources of UV and VUV laser radiation, the energy levels of the other lanthanide ions in the VUV region have to be known accurately. In the last years a lot of research has been performed on the elucidation of the high energy levels of RE ions. This was also stimulated when more high intensity VUV excitation sources like synchrotron radiation became available. For example for Gd^{3+} the VUV levels within the $4f^7$ configuration have been elucidated [6].

In the literature there has not been reported much on high energy levels of the trivalent holmium ion. The high energy transmission spectrum of $BaHo_2F_8$ has been reported by Vlasenko et al. [7], but it was recorded with a rather low resolution. Still about 15 absorption peaks in the (V)UV region of the spectrum were observed and assigned to (groups of) multiplets. In this paper we report on the VUV excitation and emission spectra of Ho^{3+} in $LiYF_4$ and YF_3 extending the energy level diagram of holmium into the VUV region.

2. Experimental

Powders of $LiYF_4$ and YF_3 doped with 1% Ho^{3+} were obtained by melting stoichiometric amounts of the fluorides with a Philips PH 1006/13 high-frequency furnace, using a modified vertical Bridgman method. The reactants were mixed in a vitreous carbon crucible. In order to remove water and air the sample was heated overnight at 450 °C in a flow of ultrapure nitrogen. Subsequently the temperature was raised to 550 °C and SF_6 was led into the reaction chamber for 30 min to remove the last traces of water and oxygen. During the rest of the synthesis a nitrogen atmosphere was maintained. Next the temperature was raised gradually until melting of the sample was visibly observed. The melt was kept at this temperature for 30 min, followed by cooling down by slowly reducing the emitted power of the high frequency generator. The sample thus obtained was a nearly oxygen-free crystal or crystalline powder and an X-ray diffraction pattern was recorded to confirm the structure and phase purity of the sample.

Low resolution excitation and emission measurements were performed on a SPEX 1680 spectrofluorometer equipped with 0.22 m double monochromators. The spectral resolution of these spectofluorometers was about 0.5 nm. For VUV/UV excitation a D_2-lamp (Hamamatsu L1835, 150 W) fitted with a MgF_2 window was used. The excitation monochromator contained VUV-gratings blazed at 150 nm (1200 lines/mm) and Al mirrors coated with MgF_2. Excitation spectra were recorded in the range 140–350 nm and were corrected for lamp intensity using sodiumsalicylate excitation spectra as reference. To avoid absorption of VUV radiation by oxygen the lamp housing, excitation monochromator and sample chamber were flushed with nitrogen for at least 2 h prior to measurements.

The emission monochromator was equipped with gratings blazed at 500 nm (1200 lines/mm). The signal was detected with a cooled Hamamatsu R928 photomultiplier tube, with which emission in the range of 250–800 nm could be measured. Emission spectra recorded with the R928 photomultiplier tube were corrected for the monochromator and for the detector response using correction spectra provided by the manufacturer. The sample temperature could be varied between liquid helium and room temperature. For the low temperature measurements an Oxford Instruments liquid helium flow cryostat, equipped with MgF_2 windows was used.

High resolution excitation spectra and low resolution VUV/UV/Vis emission spectra and decay times were measured at the HIGITI setup of the HASYLAB Synchrotron-strahlungslabor at DESY in Hamburg. For a detailed description of this setup, see [6]. The excitation monochromator consisted of a Wadsworth 1 m monochromator with a holographic MgF_2-coated Al grating blazed at 150 nm (1200 lines/mm), providing an ultimate resolution of 0.3 Å. Excitation was possible in the range 80–400 nm. Low resolution VUV/UV emission measurements were carried out using a Hamamatsu 1645U-09 channelplate detector attached to a 0.4 m Seya-Namioka monochromator with a holographic MgF_2-coated grating blazed at

150 nm (1200 lines/mm). For low resolution emission measurements in the UV/Vis region two detectors were available. Emission spectra in the range of 250–1080 nm were recorded using a Tektronix CCD array attached to a monochromator with a 150 and a 1200 lines/mm grating. Emission could also be measured in the region 300–700 nm using a cooled Hamamatsu R943-02 photomultiplier tube. The spectral resolution of both detection systems is about 1 nm. Decay times were measured using a TAC (time to amplitude converter) on a 20 ns and a 200 ns scale.

The temperature of the sample could be varied between liquid helium temperature and room temperature. The pressure in the sample chamber was maintained below 10^{-8} mbar.

3. Results and discussion

3.1. $LiYF_4:Ho^{3+}$

In Fig. 1 the high resolution excitation spectrum is presented of a $LiYF_4:Ho^{3+}$ 2% single crystal while monitoring all visible emissions. Most of the lines could be attributed to transitions from the ground state to high energy $4f^{10}$ levels of holmium and are listed in Table 1. Excitation lines due to impurities are indicated in the figure. To identify the excited states energy level calculations were performed and the assignments are included in Table 1. The parameters used for the energy level calculations (from [8]) are given in Table 2.

In the excitation spectrum of $LiYF_4:Ho^{3+}$ about 30 sharp lines corresponding to Ho^{3+} f–f transitions can be identified, in addition spin-allowed f–d excitation bands of the impurities Tb^{3+} and Dy^{3+} are observed. The rapid increase at the short-wavelength side of the spectrum is due to the onset of the f–d absorption of Ho^{3+}. In the inset of Fig. 1 the f–d absorption region of Ho^{3+} in $LiYF_4$ is presented.

In Table 1 the lowest and highest calculated crystal field level for each calculated multiplet, or group of multiplets in case of overlapping multiplets, is given. The $^{2S+1}L_J$ terms given in Table 1 are the ones with the largest weight content, since at high energies mixing of states occurs, usually of levels with the same J number.

It is therefore not always possible to assign an absorption to one particular multiplet. The energy levels were calculated using parameters obtained from the literature. With these parameters a good agreement between the calculated and measured

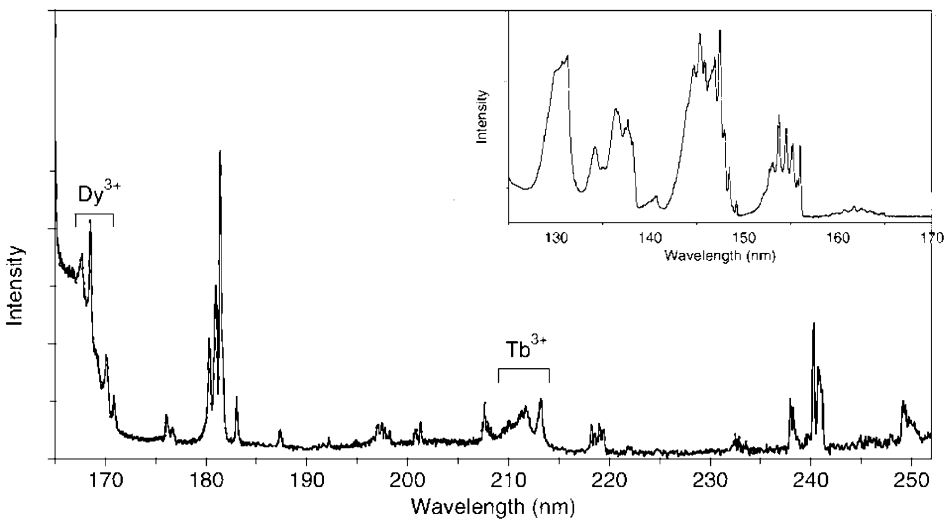

Fig. 1. Excitation spectrum of $LiYF_4:Ho^{3+}$ 2% crystal, monitoring all visible emission at 10 K. The inset shows the excitation spectrum of $LiYF_4:Ho^{3+}$ 1% powder monitoring all visible emission at 10 K.

Table 1
Experimentally observed and calculated energy levels for $LiYF_4:Ho^{3+}$ in the range 40 000–60 000 cm^{-1}

λ_{exp} (nm)	E_{exp} (cm^{-1})	Multiplets			E_{calc} (cm^{-1})	No. of levels
249.2	40 128	$^5D_1$	$^5D_3$		39 924–40 202	7
240.8	41 528				41 524–41 869	11
240.3	41 615	$^5D_4$	$^5D_2$			
238.0	42017					
		$^5D_0$			42 460	1
233.6	42 803				42 616–43 069	7
232.9	42 933	$^3F(2)_3$	$^5D_1$			
232.5	43 005					
		$^1D(3)_2$			45 166–45 196	4
219.5	45 558				45 324–45 384	30
219.0	45 660	$^3M_8$	$^3H(2)_6$	$^3H(2)_4$		
218.6	45 744					
218.2	45 825					
		$^3F(3)_3$			47 584–47 817	5
208.3	48017				47 927–48 269	8
207.9	48 093	$^3H(2)_5$				
207.7	48 149					
		$^1D(2)_2$			48 954–49 028	4
201.3	49 677	$^1H(1)_5$			49 696–49 756	8
200.8	49 796					
198.3	50 441				50 278–50 925	18
197.8	50 564	$^1K_7$	$^1G(4)_4$			
197.4	50 648					
197.1	50 743					
		$^3G(1)_3$			51 215–51 251	5
192.2	52 026	$^3G(1)_4$			51 909–52 070	7
		$^3F(4)_2$			52 995–53 058	4
187.4	53 362	$^3H(2)_6$			53 315–53 428	10
183.0	54 636	$^3F(2)_4$			54 542–54 735	7
181.7	55 039				54 957–55 317	21
181.4	55 124	$^3K(1)_8$	$^3G(1)_5$			
181.0	55 255					
180.3	55 469					
176.7	56 609	$^3H(3)_6$	$^1N_{10}$	$^3F(2)_3$	56 294–57 306	31
176.1	56 792					
		$^3F(3)_2$			57 525–57 885	4
170.4	58 517	$^3K(1)_7$			58 435–58 716	11
		$^3K(1)_6$			58 851–59 066	10
		$^3H(3)_4$	$^3H(3)_5$		60 542–60 830	15
		$^3P(1)_2$			62 970–63 048	4

Table 2
Free-ion and crystal-field parameters used for the energy level calculation of $LiYF_4:Ho^{3+}$ (in cm^{-1}) [8]

F^0	47 870	T^2	400	B_0^2	−558
F^2	96 460	T^3	37	B_0^4	−710
F^4	67 728	T^4	107	B_4^4	942
F^6	47 656	T^6	−264	B_0^6	23
α	16.1	T^7	316	B_4^6	−860
β	−529	T^8	336		
γ	1800	ζ	2148		

positions for energy levels is obtained. The presently measured new levels in the VUV may also be used to improve the parameters obtained in [8] based on a smaller number of experimental levels.

The experimentally observed levels listed in Table 1 correspond well with the regions in which energy levels are calculated. In addition to that, in regions where energy gaps with no $4f^{10}$ levels are calculated, e.g. 43 100–45 100 cm^{-1}, no f–f transitions are observed.

Usually when an energy gap is less than five times the maximum phonon energy of the host lattice, non-radiative decay becomes more probable than emission from that level and no or weak emission is observed. In the case of an energy gap that cannot be bridged by five or less phonons, emission can be observed. The maximum phonon energy of $LiYF_4$ is about 500 cm^{-1} (Li–F vibration) [9] and the energy of Y–F or Ho–F vibrations is about 400 cm^{-1}. The coupling with the Li–F vibration is relatively weak, and thus for gaps of 2000 cm^{-1} or larger emission can be expected. The energy gap between the $^1D(3)_2$ level at 45 166 cm^{-1} and $^5D_1$ at 43 069 cm^{-1} is about 2100 cm^{-1} and is thus expected to be large enough for emission from the $^1D(3)_2$ level to be observed. The energy gaps between the other levels in the region 40 000–60 000 cm^{-1} are significantly smaller, which makes multiphonon relaxation more probable than emission from those levels.

In Fig. 2 the emission spectra recorded upon excitation into the $4f^9$5d states are presented. Fig. 2(a) shows the UV emission spectrum at low temperature measured at the synchrotron and Fig. 2(b) gives the UV/visible spectrum of $LiYF_4:Ho^{3+}$ recorded at room temperature using the spectrofluorometer.

In the UV region of the spectrum transitions from the $^1D(3)_2$ level to nearly all states from $^5I_8$ to $^5F_4$ are present. In addition to that, emissions from the $^3D(1)_3$ (~33 100 cm^{-1}), $^5F_3$ (~20 600 cm^{-1}) and $^5S_2$ (~18 400 cm^{-1}) levels are observed, which is in agreement with the presence of energy gaps of 2000 cm^{-1} or more below these levels.

Quantum cutting via the sequential emission of two visible photons starting from the $^1D(3)_2$ level is possible, but only with a low visible quantum efficiency since the $^1D(3)_2$ emissions are very weak and the strongest lines are situated in the UV.

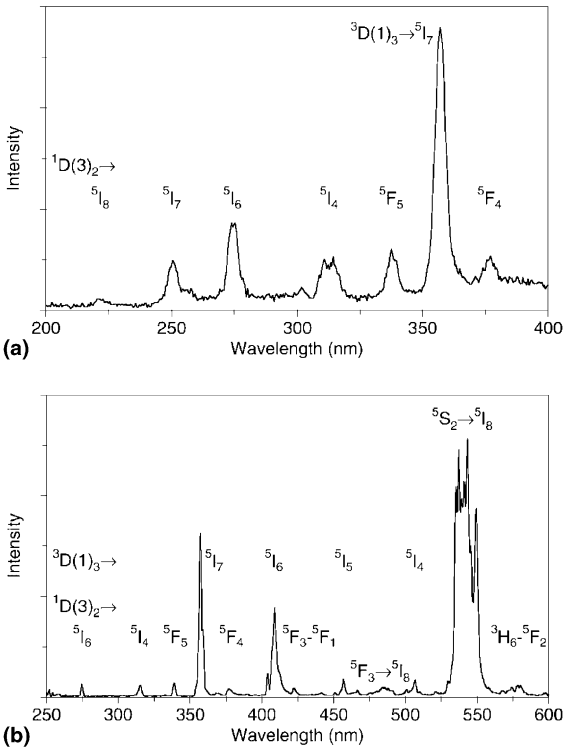

Fig. 2. (a) UV emission spectrum of $LiYF_4:Ho^{3+}$ 2% upon $4f^9$5d excitation (156 nm) at 7 K. (b) UV/visible spectrum of $LiYF_4:Ho^{3+}$ 2% upon $4f^9$5d excitation (154 nm) at 300 K.

3.2. $YF_3:Ho^{3+}$

In $LiYF_4$ the onset of the $4f^9$5d band is situated below the position calculated for the $^3P(1)_2$ level. The energy level calculations in Table 1 show that the energy between the lower $^3P(1)_2$ level and the next lower $^3H(3)_5$ levels is over 2000 cm^{-1}. Thus emission from the $^3P(1)_2$ level can possibly be observed for Ho^{3+} in a host lattice where the onset of the $4f^9$5d levels is situated at higher energies than the $^3P(1)_2$ level.

In Fig. 3 the excitation spectrum of $YF_3:Ho^{3+}$ (1%) at 10 K monitoring $^3D_3 \rightarrow {}^5I_7$ emission at 357 nm is presented. In the excitation spectrum the onset of the spin forbidden and spin allowed $4f^{10} \rightarrow 4f^9$5d transitions are situated at 155 and 148 nm, respectively.

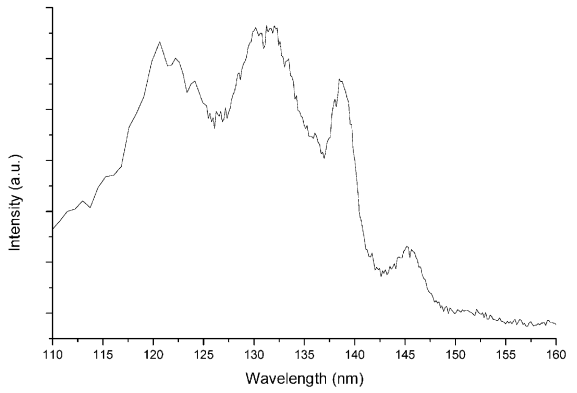

Fig. 3. Excitation spectrum of YF_3:Ho^{3+} (1%) at 10 K monitoring $^3D_3 \rightarrow {}^5I_7$ emission at 357 nm.

For $LiYF_4$:Ho^{3+} the onset of the spin forbidden and spin allowed $4f^{10} \rightarrow 4f^9 5d$ transition are reported by Wegh and Meijerink [10] to be 165 and 156 nm respectively. The situation is schematically depicted in Fig. 4. As a result of the high energy position of the lowest $4f^9$d band, emission from the $^3P(1)_2$ level may be observed for YF_3. The $^3P(1)_2$ level was calculated by Hölsä et al. to be at 62970 cm^{-1} (159 nm) and is thus situated just below the spin forbidden $4f^9 5d$ band in YF_3 and is overlapped by the spin forbidden $4f^9 5d$ band in $LiYF_4$.

In Fig. 5 the VUV/UV emission spectra of YF_3 and $LiYF_4$ doped with 1% Ho^{3+} are shown upon $4f^9 5d$ excitation at 130 nm at 10 K. Both spectra show emission peaks which originate from the $^1D(3)_2$ and $^3D(1)_3$ levels of holmium at very similar wavelengths. In addition there are several emissions marked with an arrow, which only occur in the YF_3 sample and can be attributed to emissions from the $^3P(1)_2$ level. In Table 3 an overview of assignments is given for the emissions observed in the UV region of the spectrum.

For holmium also two weak emissions in the VUV region of the spectrum were observed, at 158 nm in YF_3 and at 167 nm in $LiYF_4$ (see Fig. 5). These emissions may be attributed to spin forbidden $4f^9 5d$ emissions to the ground state. For the 158 nm emission in YF_3 the decay time was measured and a decay time of 2 ns was determined. The decay curve is shown in Fig. 6. Although it is a spin forbidden transition, the decay time is short

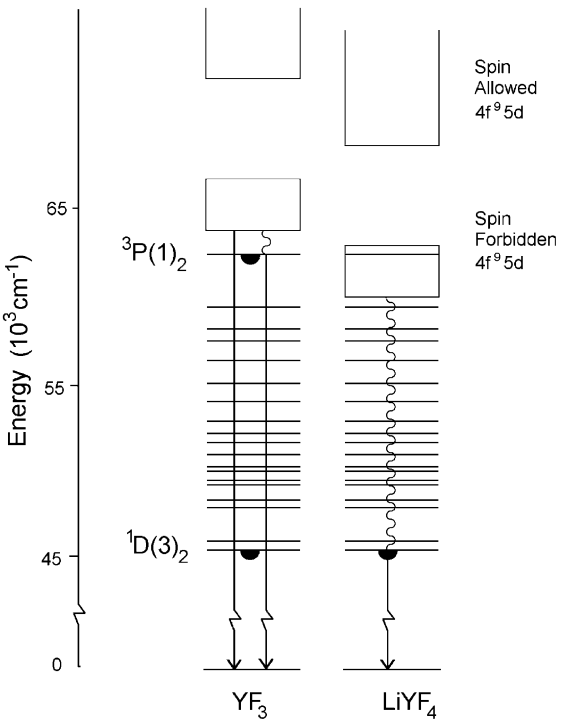

Fig. 4. Position of the $^3P(1)_2$ level with respect to the $4f^9 5d$ band in YF_3 and $LiYF_4$ (note the break in the energy scale).

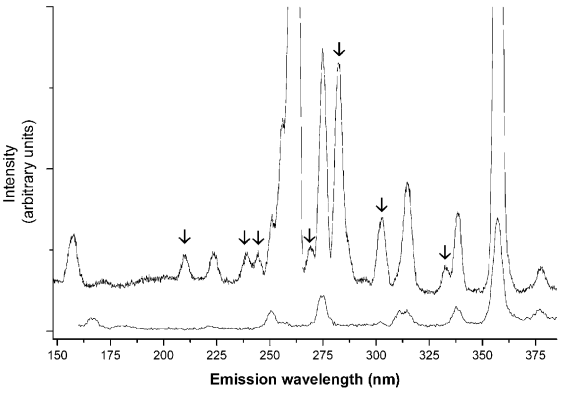

Fig. 5. Emission spectra of YF_3 (upper trace) and $LiYF_4$ (lower trace) doped with 1% Ho^{3+} upon excitation at 130 nm at 10 K. The off-scale peak at 260 nm is a second order peak.

due to the fast nonradiative relaxation to the $^3P(1)_2$ level. The decay time of the 167 nm emission in $LiYF_4$ has not been measured.

Table 3
UV emissions of Ho^{3+} in YF_3 and $LiYF_4$ upon $4f^9 5d$ excitation (130 nm)

Wavelength (nm)	Wavenumber (cm^{-1})	Assignment
210.2	47 578	$^3P_2 \rightarrow {}^5F_5$
223.5	44 743	$^1D_2 \rightarrow {}^5I_8$
239.1	41 824	$^3P_2 \rightarrow {}^3K_8$
244.4	40 917	$^3P_2 \rightarrow {}^5F_1$
251.0	39 841	$^1D_2 \rightarrow {}^5I_7$
269.4	37 120	$^3P_2 \rightarrow {}^5G_4$
274.9	36 377	$^1D_2 \rightarrow {}^5I_6$
282.2	35 436	$^3P_2 \rightarrow {}^3H_6$
302.6	33 047	$^3P_2 \rightarrow {}^3K_6$
315.0	31 746	$^1D_2 \rightarrow {}^5I_4$
332.5	30 075	$^3P_2 \rightarrow {}^3D_3$
338.6	29 533	$^1D_2 \rightarrow {}^5F_5$
357.0	28 011	$^3D_3 \rightarrow {}^5I_7$
377.0	26 525	$^1D_2 \rightarrow {}^5F_4/{}^5S_2$

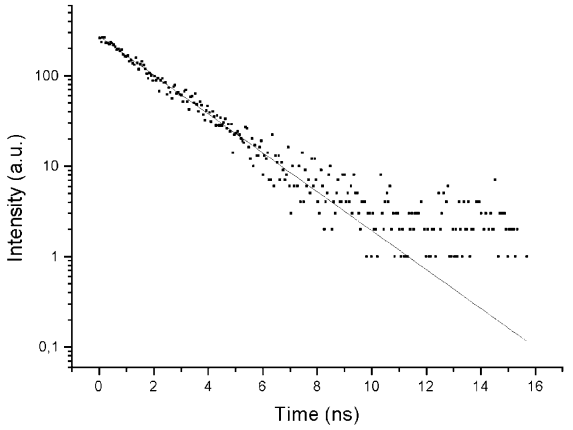

Fig. 6. Decay curve for the 158 nm emission in YF_3 at 10 K ($\lambda_{exc} = 130$ nm).

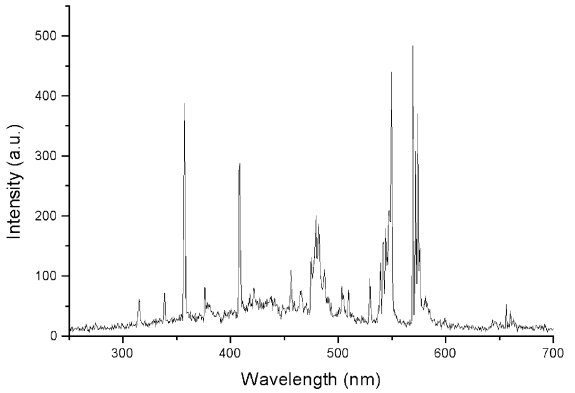

Fig. 7. Emission spectrum of YF_3:Ho^{3+} upon $4f^9 5d$ excitation at 10 K.

Table 4
Assignment of the visible emission lines for Ho^{3+} in YF_3 at 10 K upon $4f^9 5d$ excitation at 140 nm

Wavelength (nm)	Transition
357.3	$^3D(1)_3 \rightarrow {}^5I_7$
376.0	$^1D(3)_2 \rightarrow {}^5F_4$
408.5	$^3D(1)_3 \rightarrow {}^5I_6$
418.0	$^1D(3)_2 \rightarrow {}^3K(2)_8$
421.6	$^5G_5 \rightarrow {}^5I_8$
455.7	$^3D(1)_3 \rightarrow {}^5I_5$
474.8	$^1D(3)_2 \rightarrow {}^5G_5$
479.0–485.0	$^5F_3 \rightarrow {}^5I_8$
487.3	$^5G_4 \rightarrow {}^5I_7$
502.9	$^3D(1)_3 \rightarrow {}^5I_4$
509.5	$^1D(3)_2 \rightarrow {}^5G_4$
529.5	$^5G_5 \rightarrow {}^5I_7$
539.5–549.5	$^5S_2 \rightarrow {}^5I_8$
569.2–573.7	$^3D(1)_3 \rightarrow {}^5F_5$
582	$^5G_4 \rightarrow {}^5I_6$
640.0–666.0	$^5F_5 \rightarrow {}^5I_8$

3.3. Photon cascade emission

In Fig. 7 the emission spectrum upon $4f^9 5d$ excitation at 10 K of YF_3:Ho^{3+} in the visible part of the spectrum is shown. Assignments for the transitions are tabulated in Table 4. For comparison see also the emission spectrum of $LiYF_4$:Ho^{3+} (Fig. 2).

The most intense emissions are those that originate from the $^3D(1)_3$ and the $^5S_2$ level. Combining the data from Tables 3 and 4 and the emission spectra shows that photon cascade emission on holmium is possible. There is, however, no combination of two intense emissions possible, so only quantum cutting with a low visible quantum yield is observed. Examples of multi photon emission processes are: $^3P(1)_2 \rightarrow {}^3D(1)_3$ (332.5 nm), followed by $^3D(1)_3$ emissions (357, 409, 456, 503, 570 nm), or $^3P(1)_2 \rightarrow {}^5G_4$ (269 nm) followed by $^5G_4$ emissions (487, 582 nm). There is even a three photon emission process converting one VUV photon into three UV/Vis photons albeit with an estimated quantum efficiency below 0.5%: First $^3P(1)_2 \rightarrow {}^3D(1)_3$ (332.5 nm), followed by $^3D(1)_3 \rightarrow {}^5F_5$ (570 nm) and finally $^5F_5 \rightarrow {}^5I_8$ (650 nm).

4. Conclusions

The high energy levels of the Ho^{3+} ion were calculated and measured for Ho^{3+} in $LiYF_4$ and YF_3, extending the energy level diagram into the VUV region. Some high energy emissions that have not been previously reported were observed for the trivalent holmium ion. They could be attributed to spin forbidden $4f^9 5d \rightarrow 4f^{10}$ emission in YF_3 and $LiYF_4$. Emissions from the $^3P(1)_2$ level (situated around 63 000 cm^{-1}) were observed in YF_3 only, where the $^3P(1)_2$ level is situated below the $4f^9 5d$ band onset. Furthermore, several photon cascade emission processes on the holmium ion are observed including a three step process converting one VUV photon into two or three UV/Vis photons. The efficiency of the photon cascade emissions yielding visible photons is low and Ho^{3+} is not a good candidate for a commercial VUV phosphor with a visible quantum efficiency exceeding unity.

References

[1] P. Dorenbos, J. Lumin. 91 (2000) 91.
[2] G. Blasse, B.C. Grabmaier, Luminescent Materials, Springer, Berlin, 1994 (Chapter 6).
[3] T. Jüstel, J.C. Krupa, D.U. Wiechert, J. Lumin. 93 (2001) 179.
[4] H. Donker, R.T. Wegh, A. Meijerink, J.C. Krupa, M. Queffelec, J. Soc. Inf. Disp. 6 (1998) 73.
[5] R.T. Wegh, H. Donker, K.D. Oskam, A. Meijerink, Science 283 (1999) 663.
[6] R.T. Wegh, H. Donker, A. Meijerink, R.J. Lamminmäki, J. Hölsä, Phys. Rev. B 56 (1997) 13841.
[7] A.A. Vlasenko, L.I. Devyatkova, O.N. Ivanova, V.V. Mikhailin, S.P. Chernov, T.V. Uvarova, B.P. Sobolev, Sov. Phys. Dokl. 30 (1985) 395.
[8] C.K. Jayasankar, M.F. Reid, F.S. Richardson, Phys. Stat. Sol. (b) 155 (1989) 559.
[9] S.A. Miller, H.E. Rast, H.H. Caspers, J. Chem. Phys. 52 (1970) 4172.
[10] R.T. Wegh, A. Meijerink, Phys. Rev. B. 60 (1999) 10820.